Author/s:
Hewavisenti, RV;Ferguson, AL;Gasparini, G;Ohashi, T;Braun, A;Watkins, TS;Miles, JJ;Elliott, M;Sierro, F;Feng, CG;Britton, WJ;Gebhardt, T;Tangye, S;Palendira, U

Title:
Tissue-resident regulatory T cells accumulate at human barrier lymphoid organs

Date:
2021-09-01

Citation:
Hewavisenti, R. V., Ferguson, A. L., Gasparini, G., Ohashi, T., Braun, A., Watkins, T. S., Miles, J. J., Elliott, M., Sierro, F., Feng, C. G., Britton, W. J., Gebhardt, T., Tangye, S. & Palendira, U. (2021). Tissue-resident regulatory T cells accumulate at human barrier lymphoid organs. Immunology and Cell Biology, 99 (8), pp.894-906. https://doi.org/10.1111/imcb.12481.

Persistent Link:
https://hdl.handle.net/11343/298785

Tissue-resident regulatory T cells accumulate at human barrier lymphoid organs

Rehana V. Hewavisenti[1,2*], Angela L. Ferguson[1,2,3*], Georgia Gasparini[1], Tomoki Ohashi[1], Asolina Braun[4], Thomas S. Watkins[5], John J. Miles[5], Michael Elliott[6,7], Frederic Sierro[8,1], Carl G Feng[1,2,3], Warwick J Britton[2,6], Thomas Gebhardt[4], Stuart Tangye[9,10] and Umaimainthan Palendira[1,2,3]

1. School of Medical Sciences, Faculty of Medicine and Health, The University of Sydney, Sydney, NSW, Australia
2. Centenary Institute, The University of Sydney, Sydney, NSW, Australia
3. Charles Perkins Centre, The University of Sydney, Sydney, NSW, Australia
4. Department of Immunology and Microbiology, The University of Melbourne, the Peter Doherty Institute for Infection and Immunity, Melbourne, Victoria, Australia
5. Australian Institute of Tropical Health and Medicine, James Cook University, Cairns, QLD, Australia
6. Sydney Medical School, Faculty of Medicine and Health, University of Sydney, Sydney, NSW, Australia
7. Chris O'Brien Lifehouse Cancer Centre, Royal Prince Alfred Hospital, Sydney NSW, Australia
8. Australian Nuclear Science and Technology Organisation, Sydney, NSW, Australia.
9. Garvan Institute of Medical Research, Darlinghurst, NSW, Australia
10. St Vincent's Clinical School, UNSW Sydney, Darlinghurst, NSW, Australia

* Equal contributions

Running head: Resident-regulatory T cells in human lymphoid organs.

Corresponding author: Umaimainthan Palendira, Department of Infectious Diseases and Immunology, School of Medical Sciences, Faculty of Medicine and Health, The University of Sydney, Australia Telephone: +61286276115, Email: umaimainthan.palendira@sydney.edu.au

This is the author manuscript accepted for publication and has undergone full peer review but has not been through the copyediting, typesetting, pagination and proofreading process, which may lead to differences between this version and the Version of Record. Please cite this article as doi: 10.1111/IMCB.12481

Keywords: Tissue-resident memory T cells, Tregs, TFR, TFH cells

Abstract

Regulatory T cells (Tregs) play a critical role in immune regulation and peripheral tolerance. While different types of Tregs have been identified in both mice and humans, much of our understanding about how these cells maintain immune homeostasis is derived from animal models. In this study, we have examined two distinct human lymphoid organs to understand how repeated exposure to infections at mucosal surface influences the phenotype and tissue localization of Tregs. We show that while Tregs in both tonsils and spleen express a tissue-resident phenotype, they accumulate in greater numbers in tonsils. Tonsillar-resident Tregs exhibit a highly suppressive phenotype with significantly increased expression of CD39, ICOS and CTLA-4 compared to their counterparts in circulation or the spleen. Functionally, resident Tregs are able to effectively suppress T cell proliferation. We further demonstrate that tonsillar- resident Tregs share key features of T follicular helper cells. Spatial analysis reveals that the vast majority of resident Tregs are localized at the border of the T-zone and B cell follicle, as well as, within the lymphocyte pockets enriched with resident memory T cells. Together our findings suggest that resident Tregs are strategically co-localized to maintain immune homeostasis at sites of recurrent inflammation.

INTRODUCTION

Skin and mucosal sites have specific physiological functions and are continually exposed to environmental challenges. The immune system in these microenvironments encounter high levels of diverse antigenic exposure and has a distinct challenge to tolerate food or commensal antigens while avoiding persisting and recurrent infections. Tonsils are lymphoid tissues, that in humans, are lymphoepithelial organs, whose function is to survey inhaled and ingested antigens, the oral cavity microbiome, as well as respond to recurring infections[1].

Balancing between pathogen control and immune homeostasis requires coordinated responses that maximize antimicrobial effector functions while minimizing tissue damage. How such mechanisms work in humans has not been fully elucidated. Regulatory T cells (Tregs) play a critical role in maintaining tissue homeostasis by down-regulating immune responses to antigens[2]. The transcription factor forkhead box P3 (FoxP3) is critical for Treg development and its expression was initially thought to uniquely identify these cells[2]. The importance of Tregs is exemplified by loss of function mutations in *FOXP3* in patients who suffer from the often-fatal

autoimmune disease immunodysregulation polyendocrinopathy enteropathy X-linked syndrome (IPEX), as well as in Scurfy mice, which rapidly succumb to a lymphoproliferative syndrome[3–5]. Understanding how Tregs contribute to immune homeostasis in humans is therefore critical for mechanistic understanding and therapeutic development.

Different subsets of Tregs have been identified in mice and humans[6]. The first study to show that Tregs from lymphoid organs could suppress antibody production by germinal center (GC) B cells was performed on human tonsils[7]. They showed that $CD69^-$ Tregs in the tonsils were vastly superior at suppressing B cells when compared to total Tregs. Interestingly, these $CD69^-$ Tregs were shown to localize at inter-follicular regions and GCs despite the fact they expressed much lower levels of C-X-C motif chemokine receptor 5 (CXCR5) when compared to $CD69^+$ Tregs[7]. Additionally, a subset of Tregs in lymphoid organs have been identified to display a number of characteristics of T follicular helper (TFH) cells. These T follicular regulatory (TFR) cells are able to regulate both B cells and TFH cells in GCs[7–9]. Compared to other Tregs, TFR cells ($CD4^+CD25^+FoxP3^+$) express higher levels of CXCR5, BCL6, ICOS and PD-1, and secrete large amounts of immunosuppressive IL-10[10,11]. Their development, however, is dependent on GC B cells[10]. Although circulating $CXCR5^+$ Tregs have also been termed TFR cells[12], whether they are the same populations identified in lymphoid organs remains unclear[13,14]. Indeed, there are significant phenotypic and functional differences between circulating $CXCR5^+$ Tregs and TFR cells in lymphoid organs[11,13].

It has recently become evident that local immunity to persisting or recurrent infections relies on non-recirculating memory T cells that take up residence in both lymphoid and non-lymphoid tissues. These cells, termed tissue-resident memory T (Trm) cells are strategically located at sites of reinfection or pathogen reactivation, and play a critical role in controlling these infections[15]. In this regard, we showed that a significant proportion of Epstein-Barr virus (EBV) specific T cells in human tonsils express tissue-resident phenotypes, including expression of CD69 and CD103, and downregulation of tissue-exit receptors, such as Sphingosine-1-phosphate receptor 1 (S1PR1). It is still unknown whether Tregs develop residency in lymphoid organs. However, if this is the case, their contribution to tissue homeostasis requires further elucidation.

In this study, we have examined FoxP3$^+$ Tregs in two distinct human lymphoid organs, namely the tonsils and spleen, to determine how recurrent exposure to antigens impact their phenotype, function, and location. We found that a significant proportion of Tregs in these organs express a Trm T cell phenotype. These resident Tregs in tonsils also express a highly suppressive phenotype and are able to effectively suppress T cell proliferation. Interestingly, these resident Tregs possess features of TFH cells and localize mostly at the T-B border. Furthermore, we show that a greater proportion of Tregs in tonsils express a tissue-resident phenotype compared to those in the spleen, suggesting that accumulation of resident Tregs could be critical for tissue homeostasis at barrier lymphoid organs.

RESULTS

The majority of CD4$^+$ T cells in human tonsil and spleen express tissue-resident phenotype

We examined tissue-resident CD4$^+$ T cells in human tonsils and spleens. In both organs, more than half of the population of CD4$^+$ T expressed CD69 (Figure 1a) but lacked expression of other T cell activation markers (Figure 1b). Additionally, there was a significantly greater proportion of CD69$^+$CD4$^+$ T cells in the tonsils when compared to the spleen (Figure 1a). Molecular analysis revealed a transcriptional down-regulation of *S1PR1* and Kruppel-like Factor 2 (*KLF2*) in CD69$^+$CD4$^+$ T cells when compared to CD69$^-$CD4$^+$ T cells (Figure 1c). Thus, the CD69$^+$KLF2^{lo}S1PR1^{lo} phenotype, together with the absence of activation markers of splenic and tonsillar CD4$^+$ T cells, is consistent with these cells being tissue-resident. When we determined the memory status of CD69$^+$CD4$^+$ T cells, it became clear that the vast majority of the CD69$^+$ T cells in the tonsils exhibited either a CCR7$^-$CD45RA$^-$ effector memory or CCR7$^+$CD45RA$^-$ central memory phenotype while in the spleen most of these cells were effector memory (Figure 1d). Next, we assessed expression of chemokine receptors that have been found to correlate with distinct subsets of Th cells. CXCR3$^+$CD4$^+$ T cells were defined as Th1-like cells, CXCR3$^-$CCR6$^-$ cells as Th2-like, CXCR5^{hi} cells as TFH cells, and CD25^{hi}CD127^{lo} cells as Tregs. This analysis revealed that TFH cells were present in significant numbers in the tonsils and were all CD69$^+$ (Figure 1e). By contrast, as previously reported[16], there were very few CXCR5^{hi} cells in healthy human spleen. Equal proportions of CD69$^+$ and CD69$^-$ cells were present within the Th1-like, Th2-like, and Treg compartments in the spleen while a higher proportion of Th2-like and Tregs expressed CD69 in the tonsils (Figure 1e). To identify the location of CD69$^+$CD4$^+$ T cells in these organs, we performed immunofluorescence staining. This showed that while there were

multiple germinal centres present in the tonsils, as previously reported[17] the spleen was largely devoid of these structures, consistent with the paucity of TFH cells in the spleens. $CD69^{+}CD4^{+}$ T cells were largely localised at the periarteriolar lymphoid sheath in the white pulp of the spleen and in clusters (lymphocyte pockets) along the T-B border in the tonsils (Figure 1f). Together, this data shows that lymphoid-tissue resident $CD4^{+}$ T cells are present in humans, and that they adopt lymphoid organ-specific functional phenotypes, proportions, and spatial distributions.

A greater proportion of regulatory T cells in tonsils are tissue-resident compared to the spleen

To further analyse lymphoid-tissue resident $CD4^{+}$ T cells in humans, we next focused on Treg phenotypes. Although circulating Tregs have been defined on the basis of a $CD25^{hi}CD127^{lo}$ phenotype, whether this was also consistent for Tregs in human lymphoid tissues is unclear. When we examined FoxP3 expression, we found that, similar to blood, $CD4^{+}CD25^{hi}CD127^{lo}$ T cells expressed the highest levels of FoxP3 relative to total $CD4^{+}$ T cells and $CD25^{-}CD127^{+}$ non-Treg cells (Figure 2a). There was no significant difference in the expression levels of FoxP3 between $CD69^{+}$ and $CD69^{-}$ Tregs in either the tonsils or the spleen (Figure 2b). In order to determine whether the expression of CD69 on Tregs was associated with recent T cell activation, we examined for the expression of early (CD134, CD137) and late (HLA-DR) activation markers. Both CD134 and CD137 are transiently expressed upon TCR stimulation. Neither in the spleen nor in the tonsils, were there any significant differences in the expression of CD134 or CD137 or HLA-DR between $CD69^{+}$ Tregs and $CD69^{-}$ Tregs (Figure 2c), suggesting that the expression of CD69 on Tregs in these tissues is unlikely due to recent TCR stimulation. We next determined the proportions of resident ($CD69^{+}$) and circulating ($CD69^{-}$) Tregs in both the tonsils and spleen. This showed that there were significantly more tissue-resident Tregs in the tonsils compared to circulating Tregs; however, both circulating and resident Tregs were equally distributed in the spleen (Figure 2d).

Tonsillar-resident Tregs are better equipped for suppression than their splenic counterparts

Tregs exert their suppressive functions through several molecular mechanisms. We next determined differential expression of effector molecules that enable Tregs to supress immune responses. More than half of the Treg population in tonsils and spleen expressed CD39, an ectonucleotidase that facilitates the breakdown of ATP to adenosine and thereby enables

Tregs to metabolically regulate immune responses. Within organs, there were no significant differences in the proportion of $CD39^+$ tissue-resident Tregs and circulating Tregs (Figure 3a). The level of expression of CD39, however, was increased in tonsillar Tregs when compared to their splenic counterparts (Figure 3a). Expression of Inducible costimulator (ICOS) by Tregs has been associated with production of large amounts of IL-10 and enhanced suppression[18–20]. When we assessed ICOS expression, it was clear that tonsillar-resident Tregs expressed significantly higher levels of ICOS than $CD69^-$ Tregs or counterparts in the spleen (Figure 3b). Even within the spleen, resident Tregs expressed higher levels of ICOS than their $CD69^-$ circulating counterparts. Mirroring the expression of ICOS, intracellular cytotoxic T-lymphocyte-associated protein 4 (CTLA-4) expression was also significantly higher in tonsillar-resident Tregs when compared to their circulating counterparts or splenic Tregs (Figure 3c). Interestingly, not all receptors associated with Treg functions were uniformly upregulated on resident Tregs. Glucocorticoid-induced tumour necrosis factor-related receptor (GITR) is associated with the regulation of Treg function, and is thought be constitutively expressed by all Tregs [21,22]. We found all Tregs in tonsils and spleen expressed GITR, and there were no differences in the expression levels between tissue-resident and circulating Tregs (Figure 3d). Together our data shows that, when compared to their circulating counterparts, tissue-resident Tregs in human lymphoid organs are better equipped for immune regulation, and those adaptations are further strengthened at sites of recurrent antigen exposure.

Tissue-resident Tregs effectively suppress T cell proliferation

Tregs are superior at suppressing immune responses and therefore we next examined the ability of tonsular Tregs to suppress T cell proliferation *in vitro*. Isolated $CD69^+$ and $CD69^-$ Tregs from the tonsils were co-cultured at different ratios with purified CellTrace Violet (CTV) labelled $CD8^+$ T cells, which were then stimulated with T cell activation and expansion beads. After 5 days of culture, $CD8^+$ T cell proliferation was measured based on the dilution of CTV. This showed that both $CD69^+$ and $CD69^-$ Tregs effectively suppressed $CD8^+$ T cell proliferation at 1:2, 1:5 and 1:10 ratios (Figure 4). At 1:5 ratio, $CD69^+$ Tregs were able to suppress $CD8^+$ T cell proliferation by 74.5% (n = 3) compared to 47.2% (n = 3) by the $CD69^-$ Treg. There were, however, no differences in the suppression of T cell proliferation between $CD69^+$ and $CD69^-$ Treg populations at 1:2 or 1:10 ratios in suppressing $CD8^+$ T cell proliferation (Figure 4). These data demonstrate that tissue-resident Tregs can effectively supress T cell proliferation.

Tissue-resident regulatory T cells possess features of follicular regulatory T cells

We further characterised tissue-resident Tregs to determine whether they shared features of follicular regulatory T cells. As has been previously established, in the tonsils, the expression of CXCR5, a chemokine receptor that facilitates the entry of lymphocytes into B cell follicles, was highest on TFH cells (Figure 5a). Only a very small fraction of Tregs (< 2–3%) expressed CXCR5 at this level while the majority of them expressed at a moderate level. There was, however, a significant increase in CXCR5 levels on $CD69^+$ Tregs when compared to $CD69^-$ Tregs in the tonsils, but not in the spleen (Figure 5b). We then followed the gating strategy recently published by Sayin *et al*., to define TFR cells as $PD\text{-}1^{hi}CD39^+CD25^+CXCR5^+$ or $PD\text{-}1^{lo}CD39^+CD25^+CXCR5^+$ populations (Figure 5c). Comparison of the phenotypes of TFH, TFR and resident/circulating Tregs, showed that TFH cells expressed the highest levels of CXCR5, programmed cell death protein 1 (PD-1) and B cell lymphoma 6 (BCL6) in the tonsils, followed by TFR cells and $CD69^+$ Tregs (Figure 5d). By contrast, CXCR5 expression on $CD69^-$ Tregs and $PD\text{-}1^-$ Tregs were low and comparable to that of naïve $CD4^+$ T cells (Figure 5d). BCL6 is considered a master regulator of both TFH cells and TFR cells; however, there were no significant differences in its expression between TFR cells and $CD69^+$ Tregs. Finally, the expression levels of ICOS were high and comparable between TFH cells, $PD\text{-}1^+$ TFR cells and $CD69^+$ Tregs (Figure 5d), while significantly lower levels of expression were seen on $CD69^-$ Tregs, $PD\text{-}1^-$ TFR cells and naïve $CD4^+$ T cells. Together, these data show that resident regulatory T cells share features of TFH cells and based the phenotypic markers investigated in this study, these Tregs are more phenotypically similar to $PD\text{-}1^+$ TFR cells than $PD\text{-}1^-$ TFR cells.

Tissue-resident Tregs localise mostly at the T-B border and in pockets with other $CD69^+$ T cells

Having established some clear differences in the phenotype of tissue-resident Tregs and circulating Tregs in tonsils, we determined their location using multiplex immunohistochemistry (mIHC) staining. In line with our flow cytometry data, this revealed that vast majority of $FoxP3^+$ Tregs in the tonsils were $CD69^+$ (Figure 6a). We then separated the tonsil into four regions, namely germinal centre (GC), B cell follicle, T-B border, and lymphocyte pockets where there was aggregation of $CD69^+$ T cells (LP) (Figure 6b). Quantitative analysis of these regions showed that both $CD69^-$ and $CD69^+$ Tregs were present at all locations; however,

proportionally they were a very small minority compared to other lymphocytes (Figure 6c). The distribution of cells in these regions confirmed a clustering of all $CD69^+CD4^+$ T cells at lymphocyte pockets along the T-B border (Figure 6c). In order to determine whether $CD69^+$ Tregs also preferentially localised within these clusters, we enumerated cells in all four regions. This showed that while $CD69^+$ Tregs were present in follicles and GCs, they were enriched along the T-B border and particularly within lymphocyte pockets (Figure 6d). These data demonstrate that in human tonsils, most resident Tregs are located outside of GCs and are localised at the T-B border, consistent with a recent study investigating human lymph node TFR cells [23].

DISCUSSION

Tonsils are a major secondary lymphoid organ, which repeatedly gets exposed to environmental stimuli, such as pathogens, allergens, and pollutants. At this site, immune responses must be tightly regulated to maintain tissue homeostasis. Here we show that in parallel to on-going accumulation of tissue-resident memory T cells, there is a subset of regulatory cells that reside within the tonsils, and may be important for tissue homeostasis. Importantly, these tissue-resident Tregs display a highly suppressive phenotype compared to their circulating counterparts, and they are effective at suppressing T cell proliferation. Spatial analysis revealed that tonsillar-resident Tregs are strategically placed at the T-B border and could therefore regulate both T and B cell responses at this important anatomical location.

Both circulating memory T cells and Trm cells play a critical role in host defence against pathogen infection. Recent work in mice[24–26] and humans[27–29], however, shows that the presence of Trm cells at sites where pathogen re-infection or reactivation occurs, provides the host with some critical advantages in controlling persisting infections. Although $CD8^+$ Trm cells have been well described, whether $CD4^+$ T cells also reside within tissues is not completely understood[30]. Resident $CD4^+$ T cells, however, have clearly been identified through the use of parabiotic mouse models, although the duration of their stay may not be as long as their $CD8^+$ T cell counterparts[31]. In this context, we reasoned that if T cell responses to persisting or recurrent infections lead to the generation of tissue-resident memory T cells, regulatory cells could also become resident in tissues during antigen exposure and could therefore accumulate at sites of recurrent exposure as tissue-resident Tregs. Here we show that a large proportion of Tregs in human lymphoid organs have a tissue-resident phenotype. We have defined residency

on the basis of CD69 expression in the absence of any other activation markers and significant down-regulation of tissue-exit molecules. Our data also show accumulation of resident Tregs at sites of recurrent antigen exposure. The phenotype of these resident Tregs reveals that they are antigen experienced ($CD45RA^-$), and they express multiple regulatory elements. It is therefore likely that along with the formation of Trm cells, there could also be an enrichment of resident Tregs. The evidence for the existence of tissue-resident Tregs is also accumulating, principally in the skin[32,33].

Tregs maintain immune homeostasis through functional suppression of immune responses and autoreactive lymphocytes[34]. They achieve this through many different mechanisms, including deprivation of IL-2, interference by CTLA-4 co-stimulation, secretion of regulatory cytokines IL-10 or TGF-β, and the generation of adenosine through CD39 expression. Tonsillar-resident Tregs expressed the highest levels of CD39, with significantly increased expression of CTLA-4 and ICOS, suggesting that these-resident Tregs are equipped to utilise numerous mechanisms to suppress immune responses. CTLA-4 can interfere with co-stimulation of effector T cells either by competing for their binding to B7 molecules or by removing costimulatory molecules from antigen presenting cells[35]. CD39 is an ectonucleotidase that is involved in the conversion of pro-inflammatory ATP molecules into anti-inflammatory adenosine molecules[36]. Expression of ICOS has also been associated with Tregs that produce large amounts of IL-10[20], and increased numbers of $ICOS^{hi}$ Tregs have been found in autoimmune conditions[37], highlighting its importance in mediating suppressive functions. Although we have found clear differences in the expression patterns of some of the receptors on Tregs in tonsils and spleen, it is worth noting that the samples were collected from different donors.

Treg populations are capable of suppressing both T cells and B cells, and have been identified in lymphoid organs[6,10]. These cells have been described as TFRs, with features of TFH cells, including increased CXCR5 expression. Although originally identified in human tonsils[7], much of our understanding of TFRs comes from mouse models. In mice, TFR cells are largely localized within GCs and can suppress GC responses. Where TFRs are localised in human lymphoid tissues has been unclear; however, a recent study shed some light on this population. Sayin *et al*. found $CXCR5^+$ Tregs largely reside at the T-B border in human mesenteric lymph nodes and those cells were also capable of suppressing TFH-mediated isotype switching by B cells *in vitro*.

Interestingly, these TFRs were heterogeneous and based on PD-1 expression, were found to comprise two distinct populations: $PD1^{hi}$ and $PD1^{lo}$[23]. There are striking similarities between PD-1^{hi} TFRs described by Sayin *et al*., and the tissue-resident Tregs we have identified and characterised in human tonsils. In addition, tissue-resident Tregs in tonsils also express BCL6, ICOS and PD-1, features commonly expressed by TFH cells, suggesting that previously described TFR cells and tissue-resident Tregs largely overlap. Whether TFR cells are a specialized subset of resident Tregs remains to be investigated. The absence of B cells leads to a significant reduction of TFR cells in lymphoid organs, while $CXCR5^+$ Tregs in blood remain unaffected[38]. In order to reconcile these differences, two models have been proposed. In the first model, circulating $CXCR5^+$ Tregs have been suggested to be the memory-like population that bypasses GC responses[38]. In the second model, the circulating $CXCR5^+$ cells are suggested to be immature TFR cells that rely on GC B cells for their full maturation[11]. One potential confounding factor in some studies that have examined TFR cell development in mice, is that these studies use a short time frame used to assess the phenotype following immunization.

The location of resident Tregs in tonsils is largely at the T-B border and in clusters with other Trm cells. This positioning may be crucial for their ability to suppress T cells, TFH cells and B cells within the lymphoid organs. Distinct clustering along with other $CD69^+$ T cells also suggests that local microenvironmental cues could be a factor in their anatomical positioning. Either antigen presenting cells or survival factors could be at the centre of these pockets. Studies in mice have shown that in a steady state, Tregs do localise in clusters with effector T cells within lymphoid organs, due to the presence of IL-2 and antigen presenting dendritic cells [39]. Whether resident Tregs in human lymphoid organs follow a similar path remains to be seen.

In conclusion, identifying a subset of Tregs that preferentially reside in tissues and contribute to local immune regulation, autoimmunity and cancer is critical. More specifically, resident-Tregs may have implications in the development or resolution of autoimmune disease, which can be organ specific. Our data show that these tissue-resident Tregs have a distinct phenotype compared to the circulatory counterparts, and could be better suited to perform local regulatory functions. This implies that this subset of Tregs could be an ideal target for regulating inflammatory conditions. Boosting their numbers in an inflammatory environment could provide an extra layer of regulation and restore peripheral tolerance. On the contrary,

these resident Tregs could also become a target for checkpoint blockade therapy. Increased expression of CTLA-4 and PD-1 by this subset suggests that checkpoint blockade therapies targeting these molecules could also target tissue-resident Tregs and lead to depletion of these local regulators.

METHODS

Human tissues and blood samples

Human spleens and blood samples were obtained from the Australian Red Cross Blood services. Buffy coats were collected from healthy donors, and spleens from cadaveric organ donors. Palatine tonsils were obtained as discarded tissue from routine tonsillectomy patients. The use of human samples in this project was approved by the relevant ethics committees affiliated with the Royal Price Alfred Hospital (RPA), St Vincent's Hospital and the Mater Hospital and were collected after informed patient consent. Tonsil and spleen samples were partially dissected for OCT preservation and formalin-fixed prior to paraffin embedding. Remaining tissue samples were processed to single-cell suspensions by pushing through a cell strainer followed by Ficoll-Hypaque (GE Healthcare, Chicago, Illinois, USA) separation to isolate the mononuclear cell layer. PBMCs were extracted from buffy coats by Ficoll separation. Cells were cryopreserved in liquid nitrogen for down-stream experimentation.

Ethics statement

This study was approved by human ethics committees of the RPA Hospital, the Mater Hospital, St Vincent's hospital and Sydney South West Area Health Services (Australia). Informed written consent was obtained for all human tissues used.

Flow cytometry analysis

Cells from blood, spleen and tonsils were thawed and were stained for cell surface and intracellular markers. Fluorochrome-conjugated antibodies (mAbs) for extracellular markers were stained for 20 min at 4°C. The following mAbs were used for phenotypic identification of $CD4^+$ T cells, regulatory T cells, $CD8^+$ T cells, Naïve, T follicular cells and T follicular regulatory T cells: anti-CD69, CD25, CD39, CD8, CTLA-4, ICOS (Biolegend, San Diego, CA, USA), CD45RA, PD-1, CD3, CD127, CD103 (BD Biosciences, San Jose, CA, USA), CCR7, CD39, CD137, HLA-DR, CXCR5, GITR, BCL6, and FoxP3 (intracellular) (all obtained from Biolegend). Transcription Factor

Buffer Set (BD Pharmingen, San Jose, CA, USA) was used for permeabilisation and intracellular staining as per manufacture instructions. Tissue-resident populations were identified using anti-CD69 (BV650 (Biolegend); FITC (BD Biosciences). Activation markers: anti-CD45RA, anti-CD134, anti-HLA-DR (all from BD Biosciences), and anti-CD137 (From Biolegend). $CD4^+$ T cells were defined as ($CD45RA^-CD3^+CD4^+$), and Tregs ($CD3^+CD4^+CD25^{hi}CD127^{lo}FoxP3^+$). Stained cells were analyzed using LSR-Fortessa (5 laser) flow cytometer (BD Biosciences) and the data processed using FACs DIVA (BD Biosciences) and FlowJo software (Treestar, Ashland, USA; v9.9.6; 10).

Immunofluorescence and multiplex Immunohistochemistry (IHC)

All spleen immunofluorescence staining was carried out on 7 μm frozen sections. Sections were acetone-fixed prior to PBS rehydration (spleens only). Tissues were blocked with 30% horse serum and stained with primary then secondary antibodies for 1 h at room temperature in the dark. The following primary mAbs were used; to identify Tregs, anti-Foxp3 (Abcam, Cambridge, UK), and to identify B cells, anti-IgM (Life Technologies, Carlsbad, CA, USA). The expression of CD69 and CD4 (to identify $CD4^+$ T cells) was identified using biotin-conjugated anti-CD69 mAb (Biolegend) and conjugated CD4-AF647 mAbs (BD Biosciences). The following secondary antibodies were used; affinity purified F(ab')2 fragments of CyTM3 conjugated donkey anti-mouse IgG and CyTM3 conjugated donkey anti-goat IgG (Jackson ImmunoResearch, West Grove, Pennsylvania, USA). Control antibodies or secondary mAbs in the absence of primary mAbs were used to determine background fluorescent levels. Images were acquired using the epifluorescence Deltavision microscope (Perkin Elmer, Waltham, Massachusetts, USA). Following acquisition, high-resolution mosaic images of the spleen were obtained by applying the stitching function of the Softworx software (GE Healthcare).

Formalin-fixed paraffin-embedded (FFPE) tonsil tissue blocks were cut at 4um thickness and stained using OPAL mIHC assay kit (PerkinElmer) as per optimised in-house protocol. Briefly, FFPE tissue sections were deparaffinized and rehydrated. Tissues were then subjected to antigen retrieval by boiling in basic (10 mmol L^{-1} Tris base, 1 mmol L^{-1} EDTA, 0.05% Tween 20, pH 9.0) buffer. Tissue sections were then incubated with 3% hydrogen peroxide for 20 min at room temperature before washing and blocking with Perkin Elmer Antibody diluent / Block buffer. Sections were then incubated with a single unconjugated primary antibody for 35 min,

washed and then incubated with Opal Polymer HRP (Akoya Biosciences, Menlo Park, CA, USA) for 10 min or MACH 2-step HRP polymer detection (mouse or rabbit) 5mins/step (Biocare Medical, Pacheco, CA, USA). After washing, sections were incubated with opal fluorochromes at a 1:100 dilution made up in tyramide signal amplification (TSA) reagent (PerkinElmer) for 10 min. The antigen retrieval step was repeated, and tissue was stained for subsequent antibodies as described above. After all staining was complete; sections were stained with DAPI (Cell Signalling Technologies, Danvers Massachusetts, USA) for 5 min, and then mounted using Prolong Diamond (Life Technologies). Slides are kept in the dark until imaging is complete. The following antibodies were used; CD4 (104R-15 clone; Cell Marque), CD69 (EPR21814 clone; Abcam) CD20 (L26 clone, Biocare Medical) and FoxP3 (Ab20034 clone; Abcam). Mantra imaging platform (PerkinElmer) was used for imaging in combination with Mantra snap software for data acquisition. For all quantitative analysis, up to 10 randomly selected regions of interest per section were analysed. Inform advanced image analysis software (PerkinElmer) was used to process and analyse images. Each tissue was manually segmented into tissue regions.

Cell sorting

For *in vitro* cultures, Treg subsets, CD8+ T cells and non-Tregs were sorted using FACS Aria cell sorter (BD Sciences). Lymphocytes were stained for anti-CD3 (UCHT1; Biolegend), anti-CD4 (RPA-T4; BD Bioscience), anti-CD25 (M-A251; BD Biosciences), anti-CD127 (A019D5; BD Biosciences), anti-CD8 (HIT8a; Biolegend) and anti-CD69 (FN50; BD Biosciences). The cells were defined as $CD4^+$ lymphocytes by selecting the $CD3^+CD4^+$ population and then further defined as Tregs by selecting $CD25^{hi}CD127^{lo}$ cells. Tregs were further differentiated into $CD69^+$ and $CD69^-$ subsets and collected. Both $CD8^+$ T cells, which were gated from within the $CD4^-CD3^+$ populations, and $CD69^-$ non-Tregs ($CD25^{lo}CD127^+$) were also collected. Purity of the sorted populations was greater than 95%.

***In vitro* suppression assays**

In vitro suppression assays were performed in 96-well round-bottom plates in medium consisting of RPMI 1640 (Buffalo, NY, USA) supplemented with 10% heat inactivated fetal calf serum (FCS), 100 U mL^{-1} penicillin (Sigma-Aldrich, St. Louis, Missouri, USA), and 100 µg mL^{-1} streptomycin (Sigma-Aldrich. All wells contained 1×10^5 $CD8^+$ T cells, and different ratios of

414 $CD69^+$ $CD127^{lo}$ Tregs, $CD69^-CD25^{hi}CD127^{lo}$ Tregs, $CD69^-CD25^{lo}CD127^+$ non-Tregs. The number
415 of these cells in wells were either 1×10^5, 5×10^4, 2×10^4, or 1×10^4, with suppressor-to-
416 responder ratios of 2:1, 5:1, or 10:1, respectively. In control cultures, $CD69^-CD25^{lo}CD127^+$ non-
417 Tregs were added instead of suppressors. CD3/CD28 T cell activation and expansion beads (TAE
418 beads, Miltenyi Biotec, Bergisch Gladbach, Germany) were used to activate $CD8^+$ T cells. They
419 were added to each well in a 1:2 (1 TAE: 2 $CD8^+$ T cells) ratio. $CD8^+$ T cells (responder cells)
420 were stained with CellTrace Violet (Thermo Fisher Scientific, Waltham, Massachusetts, USA) to
421 assess proliferation, and cell analysis was performed after 5 days in culture using flow
422 cytometry. All cells were stained with mAb for CD69 (FN50; BD Biosciences), CD3 (UCHT1;
423 Biolegend), CD4 (RPA-T4; BD Bioscience) and CD8 (HIT8a; Biolegend). Stained cell samples
424 were processed on a BD FACS Fortessa flow cytometer (BD Biosciences) and results were
425 recorded using FACSDiva (BD Biosciences). Percentage of proliferation was calculated relative
426 to the mean number of divided cells in control wells containing only responder cells. FlowJo
427 software was used to calculate the division index (DI), the average number of divisions a cell in
428 the starting population has undergone. This was then used to calculate the percentage
429 suppression: (**% Suppression** = 100 – ((DI of Treg $^+$ $CD8^+$ co-culture)/ DI of $CD8^+$ alone) x 100)[40].
430
431 **ACKNOWLEDGMENTS**
432 This project was supported by grants from the National Health and Medical Research Council
433 (NHMRC) of Australia and the NSW Government Infrastructure Grant to the Centenary
434 Institute. We thank the Australian Centre for Microscopy & Microanalysis and Sydney
435 Cytometry at the University of Sydney for their assistance with this work.
436
437 **CONFLICT OF INTEREST**
438 The authors have declared that no conflict of interest exists.
439
440
441 **REFERENCES**
442 1. Perry M, Whyte A. Immunology of the tonsils. *Immunol Today* 1998; **19:** 414–421.
443 2. Savage PA, Klawon DEJ, Miller CH. Regulatory T Cell Development. *Annu Rev Immunol*
444 2020; **38**: 421–453.
445 3. Wildin RS, Ramsdell F, Peake J, *et al*. The immune dysregulation, polyendocrinopathy,

enteropathy, X-linked syndrome (IPEX) is caused by mutations of FOXP3. *Nat Genet* 2001; **27**: 20-21.

4. Hori S, Nomura T, Sakaguchi S. Control of regulatory T cell development by the transcription factor Foxp3. *Science* 2003; **299:** 1057–1061.
5. Fontenot JD, Gavin MA, Rudensky AY. Foxp3 programs the development and function of CD4+CD25+ regulatory T cells. *Nat Immunol* 2003; **4**: 330–336.
6. Sakaguchi S, Miyara M, Costantino CM, Hafler DA. FOXP3^{+} regulatory T cells in the human immune system. *Nat Rev Immunol* 2010; **10**: 490–500.
7. Lim HW, Hillsamer P, Kim CH. Regulatory T cells can migrate to follicles upon T cell activation and suppress GC-Th cells and GC-Th cell-driven B cell responses. *J Clin Invest* 2004; **114**: 1640–1649.
8. Chung Y, Tanaka S, Chu F, *et al*. Follicular regulatory T cells expressing Foxp3 and Bcl-6 suppress germinal center reactions. *Nat Med* 2011; **17**: 983–988.
9. Linterman MA, Pierson W, Lee SK, *et al*. Foxp3^{+} follicular regulatory T cells control the germinal center response. *Nat Med* 2011; **17**: 975–982.
10. Sage PT, Sharpe AH. T follicular regulatory cells. *Immunol Rev* 2016; **271**: 246–259.
11. Fonseca VR, Ribeiro F, Graca L. T follicular regulatory (Tfr) cells: Dissecting the complexity of Tfr-cell compartments. *Immunol Rev* 2019; **288**: 112–127.
12. Wing JB, Kitagawa Y, Locci M, *et al*. A distinct subpopulation of CD25^{-} T-follicular regulatory cells localizes in the germinal centers. *Proc Natl Acad Sci USA* 2017; **114**: E6400–E6409.
13. Fonseca VR, Agua-Doce A, Maceiras AR, *et al*. Human blood Tfr cells are indicators of ongoing humoral activity not fully licensed with suppressive function. *Sci Immunol* 2017; **2**: 1–13.
14. Maceiras AR, Fonseca VR, Agua-Doce A, Graca L. T follicular regulatory cells in mice and men. *Immunology* 2017; **152**: 25–35.
15. Gebhardt T, Palendira U, Tsharke DC, Bedoui S. Tissue-resident memory T cells in tissue homeostasis, persistent infection and cancer surveillance. *Immunol Rev* 2018; **283**: 54-76
16. Bentebibel SE, Schmitt N, Banchereau J, Ueno H. Human tonsil B-cell lymphoma 6 (BCL6)-expressing CD4^{+} T-cell subset specialized for B-cell help outside germinal centers. *Proc Natl Acad Sci USA* 2011; **108:** E488-E497.

17. Audia S, Rossato M, Santegoets K, Spijkers S, *et al*. Splenic TFH expansion participates in B-cell differentiation and antiplatelet-antibody production during immune thrombocytopenia. *Blood* 2014; **124**: 2858–2866.
18. Vocanson M, Rozieres A, Hennino A, Poyet G, *et al*. Inducible costimulator (ICOS) is a marker for highly suppressive antigen-specific T cells sharing features of TH17/TH1 and regulatory T cells. *J Allergy Clin Immunol* 2010; **126**: 280-289
19. Redpath SA, van der Werf N, Cervera AM, Macdonald AS, *et al*. ICOS controls Foxp3$^+$ regulatory T-cell expansion, maintenance and IL-10 production during helminth infection. *Eur J Immunol* 2013; **43**: 705–715.
20. Ito T, Hanabuchi S, Wang YH, Park WR, *et al*. Two Functional Subsets of FOXP3$^+$ Regulatory T Cells in Human Thymus and Periphery. *Immunity* 2008; **28**: 870–880.
21. Shimizu J, Yamazaki S, Takahashi T, Ishida Y, Sakaguchi S. Stimulation of CD25$^+$CD4$^+$ regulatory T cells through GITR breaks immunological self-tolerance. *Nat Immunol* 2002; **3**: 135–142.
22. Knee DA, Hewes B, Brogdon JL. Rationale for anti-GITR cancer immunotherapy. *Eur J Cancer* 2016; **67**: 1–10.
23. Sayin I, Radtke AJ, Vella LA, Jin W, *et al*. Spatial distribution and function of T follicular regulatory cells in human lymph nodes. *J Exp Med* 2018; **215**: 1531–1542.
24. Gebhardt T, Wakim LM, Eidsmo L, Reading PC, Heath WR, Carbone FR. Memory T cells in nonlymphoid tissue that provide enhanced local immunity during infection with herpes simplex virus. *Nat Immunol* 2009 May; **10**: 524–530.
25. Jiang X, Clark R A, Liu L, Wagers AJ, Fuhlbrigge RC, Kupper TS. Skin infection generates non-migratory memory CD8$^+$ T(RM) cells providing global skin immunity. *Nature* 2012; **483**: 227–231.
26. Shin H, Iwasaki A. A vaccine strategy that protects against genital herpes by establishing local memory T cells. *Nature* 2012; **491**: 463–467.
27. Zhu J, Peng T, Johnston C, Phasouk K, *et al*. Immune surveillance by CD8αα$^+$ skin-resident T cells in human herpes virus infection. *Nature* 2013; **497**: 494–497.
28. Jozwik A, Habibi MS, Paras A, Zhu J, *et al*. RSV-specific airway resident memory CD8$^+$ T cells and differential disease severity after experimental human infection. *Nat Commun* 2015; **6**: 10224.
29. Clark R A., Watanabe R, Teague JE, Schlapbach C, *et al*. Skin Effector Memory T Cells Do

Not Recirculate and Provide Immune Protection in Alemtuzumab-Treated CTCL Patients. *Sci Transl Med* 2012; **4**: 117ra7.

30. Carbone FR, Gebhardt T. Should I stay or should I go—Reconciling clashing perspectives on CD4+ tissue-resident memory T cells. *Sci Immunol* 2019; **4**: 8–10.
31. Beura LK, Fares-Frederickson NJ, Steinert EM, Scott MC, *et al*. $CD4^+$ resident memory T cells dominate immunosurveillance and orchestrate local recall responses. *J Exp Med* 2019; **216**: 1214–1229.
32. Rosenblum MD, Way SS, Abbas AK. Regulatory T cell memory. *Nat Rev Immunol* 2016; **16**: 90-101.
33. Ali N, Rosenblum MD. Regulatory T cells in skin. *Immunology* 2017; **152**: 372–381.
34. Vignali DAA, Collison LW, Workman CJ. How regulatory T cells work. *Nat Rev Immunol* 2008; **8**: 523–532.
35. Lucca LE, Dominguez-Villar M. Modulation of regulatory T cell function and stability by co-inhibitory receptors. *Nat Rev Immunol* 2020; **20**: 680-693.
36. Deaglio S, Dwyer KM, Gao W, Friedman D, *et al*. Adenosine generation catalyzed by CD39 and CD73 expressed on regulatory T cells mediates immune suppression. *J Exp Med* 2007; **204**: 1257–1265.
37. Herman AE, Freeman GJ, Mathis D, Benoist C. $CD4^+CD25^+$ T regulatory cells dependent on ICOS promote regulation of effector cells in the prediabetic lesion. *J Exp Med* 2004; **199**: 1479–1489.
38. Sage PT, Alvarez D, Godec J, Von Andrian UH, Sharpe AH. Circulating T follicular regulatory and helper cells have memory-like properties. *J Clin Invest* 2014; **124**: 5191–5204.
39. Liu Z, Gerner MY, Van Panhuys N, Levine AG, Rudensky AY, Germain RN. Immune homeostasis enforced by co-localized effector and regulatory T cells. *Nature* 2015; **528**: 225–230.
40. Mcmurchy AN, Levings MK. Suppression assays with human T regulatory cells: A technical guide. *Eur J Immunol* 2012; **42**: 27–34.

Figure Captions

Figure 1. Majority of $CD4^+$ T cells in human lymphoid tissues express tissue-resident

phenotype. (a) The proportion of $CD69^+CD4^+$ T cells in blood (n = 6), tonsils (n = 12) and spleen (n = 11). (**b**) $CD69^{+/-}CD4^+$ T cell subsets were analysed for the expression of activation markers HLA-DR, CD134 and CD137 from the tonsils (n = 4) **(c)** Relative expression of *S1PR1* and *KLF2* in isolated $CD69^+CD4^+$ and $CD69^-CD4^+$ T cells were analysed by RT-PCR. Individual dots represent individual donor samples (Spleen: n = 6 (*S1PR1*) and n = 5 (*KLF2*); Tonsil: n = 3 (*S1PR1*) and (*KLF2*)). The proportion of tonsillar $CD69^+CD4^+$ T cells were identified into **(d)** naïve ($CCR7^+CD45RA^+$), central memory (TCM, $CCR7^+CD45RA^-$), effector memory ($CCR7^-CD45RA^-$) and TEMRA ($CCR7^-CD45RA^+$) populations (n = 5) and **(e)** Th1-like ($CXCR3^+$), Th2-like ($CXCR3^-CCR6^-$), Treg ($CD25^+CD127^-$) and TFH ($CXCR5^{hi}$) $CD4^+$ T cell subsets (n = 4). **(f)** Immunofluorescence analysis of fresh frozen spleen (left panel) and mIHC of FFPE tonsil section (right panel) stained for CD4 (blue), CD69 (red) and splenic B cells (IgM, green) or tonsil B cells (CD20, green). Scale bars: Spleen-10 μm, Tonsil- 50 μm; n = 3. **(a)**, **(b)** and **(d)** data were analysed using flow cytometry with data depicted with error bars representing mean ± SEM. Statistical significance was determined for **(a)** and **(c)** using the non-parametric unpaired Mann-Whitney *U*-test and **(d)** ANOVA with Holm-Sidak multiple comparison test $*P < 0.05$ $**P < 0.01$ $***P < 0.001$.

Figure 2. Human tonsils are enriched with resident Tregs. Mononuclear cells isolated from human tonsils and spleen, were stained for Treg markers and examined by flow cytometry. **(a)** Tregs were gated in the tonsil (n = 14), spleen (n = 10), and blood (n = 11). $CD4^+CD3^+$ T cells were isolated, and Tregs were defined as $CD25^{hi}CD127^{lo}$ phenotype with $CD25^{lo}CD127^+$ cells were gated as non-Tregs (left panel). FoxP3 expression was assessed in $CD4^+$ T cells, Tregs and Non-Treg (right panel) populations. **(b)** FoxP3 expression levels were assessed in $CD69^+$Tregs and $CD69^-$ Tregs in both the tonsils (n = 12) and spleen (n = 8) (left and middle panels). **(c)** The expression of early (CD134, CD137) and late (HLA-DR) activation markers on Tregs were analysed between $CD69^+$ and $CD69^-$ Tregs. Graphs show the mean and SEM for tonsils (CD134 (n = 4), CD137 (n = 6), HLA-DR n = 9) and spleen (CD134 (n = 9), CD137 (n = 6), HLA-DR (n = 12)). **(d)** Quantification of the proportion of Tregs expressing CD69 in both the tonsils and spleen with data depicted as the mean and SEM for tonsils (n = 15) and spleen (n = 16). Grey shaded histograms represent unstained or fluorescence minus one (FMO) controls. Statistical significance was determined using the Kruskal-Wallis *H*-test with Dunn's multiple comparison $*P < 0.05$ $**P < 0.01$ and $***P < 0.001$.

Figure 3. Tonsillar-resident Tregs express a highly suppressive phenotype. The expression of molecules associated with the suppressive function of Tregs was determined by flow cytometry. **(a)** The proportion of $CD69^+$ and $CD69^-$ Tregs expressing CD39 was determined for the tonsils (n = 10) and spleen (n = 7) (left panel). Representative flow cytometry plot for the expression of CD39 by Tregs (right-top panels), and the mean fluorescence intensity (MFI) values for CD39 on $CD69^+$ and $CD69^-$ Tregs in the tonsils (n = 5) and spleen (n = 9). **(b)** Representative flow cytometry overlaid histogram plots (top panel) and graph showing the MFI values (bottom panel) for the expression of ICOS on Tregs from the tonsils and spleens. Grey shaded histograms represent unstained or FMO controls. Data are presented as the mean and SEM of 5 tonsils and 6 spleens. **(c)** Representative flow cytometry plots (top panels) and graphs showing the MFI values (bottom panels) for the expression of intracellular CTLA-4 on Tregs from tonsils and spleen. Data are presented as the mean and SEM of 5 tonsils and 5 spleens. **(d)** Representative flow cytometry overlaid histogram plots (top panel) and graph showing the MFI values (bottom panel) for the expression of GITR on Tregs from tonsils and spleens. Data are presented as the mean and SEM of 5 tonsils and 7 spleens. Statistical significance was determined by the non-parametric unpaired Mann-Whitney *U*-test $*P < 0.05$.

Figure 4. Resident Tregs effectively suppress T cell proliferation. The ability of Tregs from tonsils to suppress T cell proliferation was measured by co-culturing purified CTV labelled $CD8^+$ T cells with different ratios of purified $CD69^+$ or $CD69^-$ Tregs or non-Treg $CD4^+$ T cells. After 5 days of culture, flow cytometry was used to determine the proportion of T cells proliferating in culture. **(a)** Representative flow cytometry plots show the dilution of CTV by $CD8^+$ T cells co-cultured with non-Treg $CD4^+$ T cells (grey), $CD69^+$ Tregs (red) and $CD69^-$ Tregs (blue). **(b)** Graph shows the mean and SEM of the percentage suppression of $CD8^+$ T cells at different ratios. Individual dots represent individual donor cells and independent experiments. The non-parametric unpaired *t*-test Mann-Whitney *U*-test (compare ranks) were used to assess whether statistical significance was evident. It was determined that there were no significant differences.

Figure 5. Resident Tregs in tonsils possess features of follicular regulatory T cells. (a) Flow cytometry plots showing the gating strategy used to identify Tregs. Cells were gated on CD45RA-$CD4^+$ population and the top panel shows the tonsils and the bottom panel shows the

spleen. Representative histogram plot (middle panels) and graph (right) showing the MFI values for the expression of CXCR5 on Tregs in the tonsils (top panels) and spleen (bottom panels). **(b)** Gating strategy used to identify follicular regulatory T cells. **(c)** Representative flow cytometry overlaid histogram plots and graph showing the MFI values comparing TFR cells, Tregs and naive $CD4^+$ T cells for the expression of CXCR5, PD-1, BCL6 and ICOS. Data are presented as the mean and SEM of 5 tonsils. Statistical significance was determined using the Kruskal-Wallis *H*-test with Dunn's multiple comparison $*P < 0.05$, $**P < 0.01$ and $***P < 0.001$.

Figure 6. Resident Tregs localise at T-B border and in lymphocyte pockets. Quantitative mIHC staining of FFPE tissue was used to determine the location of Tregs within the tonsils. **(a)** Box and Whisker plots show the proportion of Tregs (top panel) and $CD4^+$ T cells (bottom panel) expressing CD69 by tissue staining. Statistical analysis was performed using the Wilcoxon matched pairs signed rank test $*P < 0.05$. **(b)** Representative image shows the separation of tonsil into 4 regions of interest, Germinal Centre (GC), follicle, T-B border and Lymphocyte Pockets (LP), scale bar 50 μm. In higher magnification images, the arrows point to $FoxP3^+$ (pink) $CD69^+$ (red) $CD4^+$ (green) T cells, scale bars 10 μm. **(c)** Pie charts show the proportion of different cell subsets identified by markers CD4, CD69, FoxP3, CD20 by tissue staining in whole section (All tonsils), follicles, GC, T-B border and LP. (**d)** Box and Whisker plots show the densities of different subsets of CD4+ T cells in each region. Statistical significance was determined using multiple unpaired *t*-tests $*P < 0.05$ $***P < 0.001$. **(e)** Parts-of-whole charts showing the distribution of each CD4+ T cell and Treg subset in follicles, GC, T-B border and LP.

Figure 1.

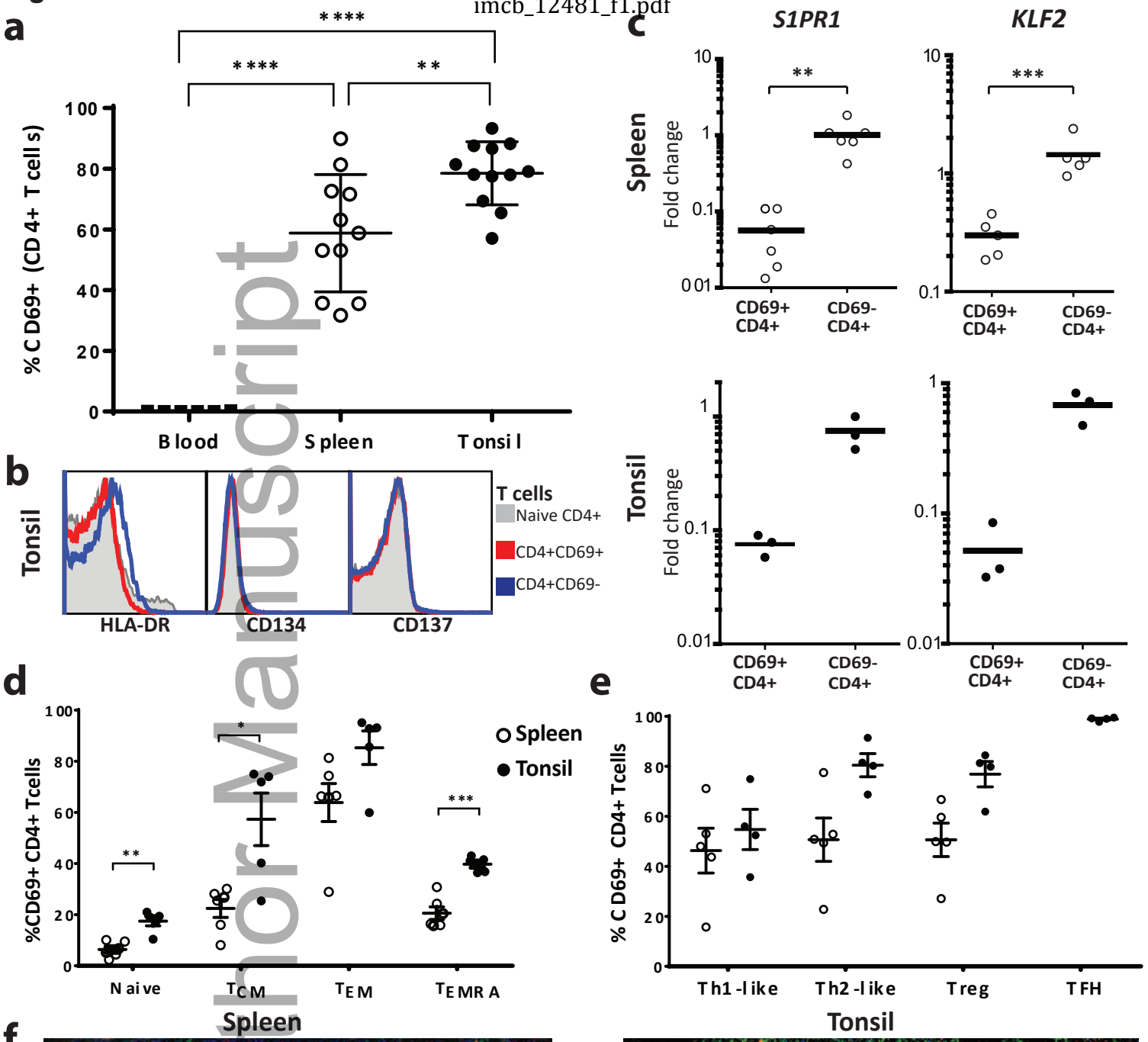

Figure 2.

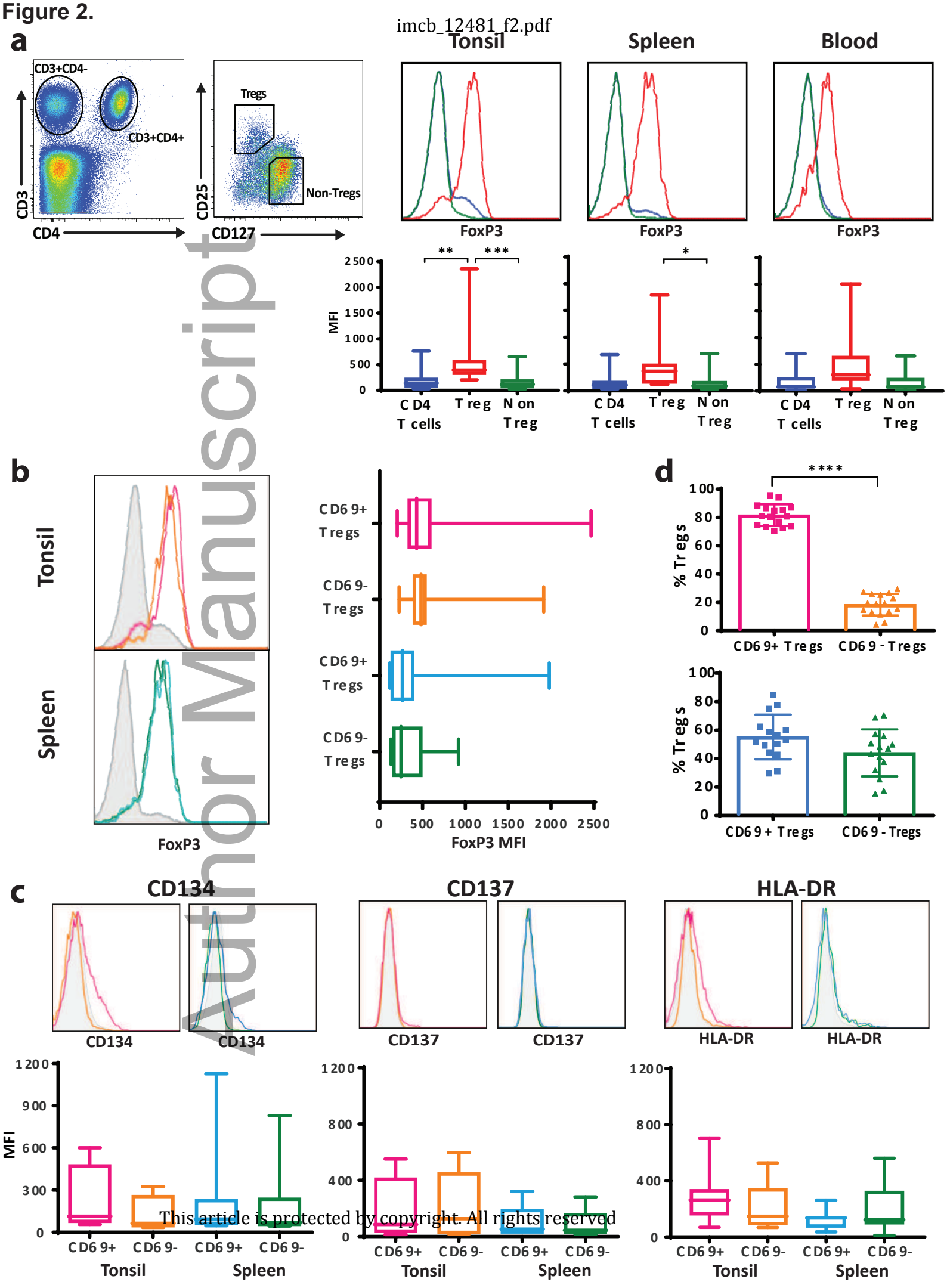

Figure 3.

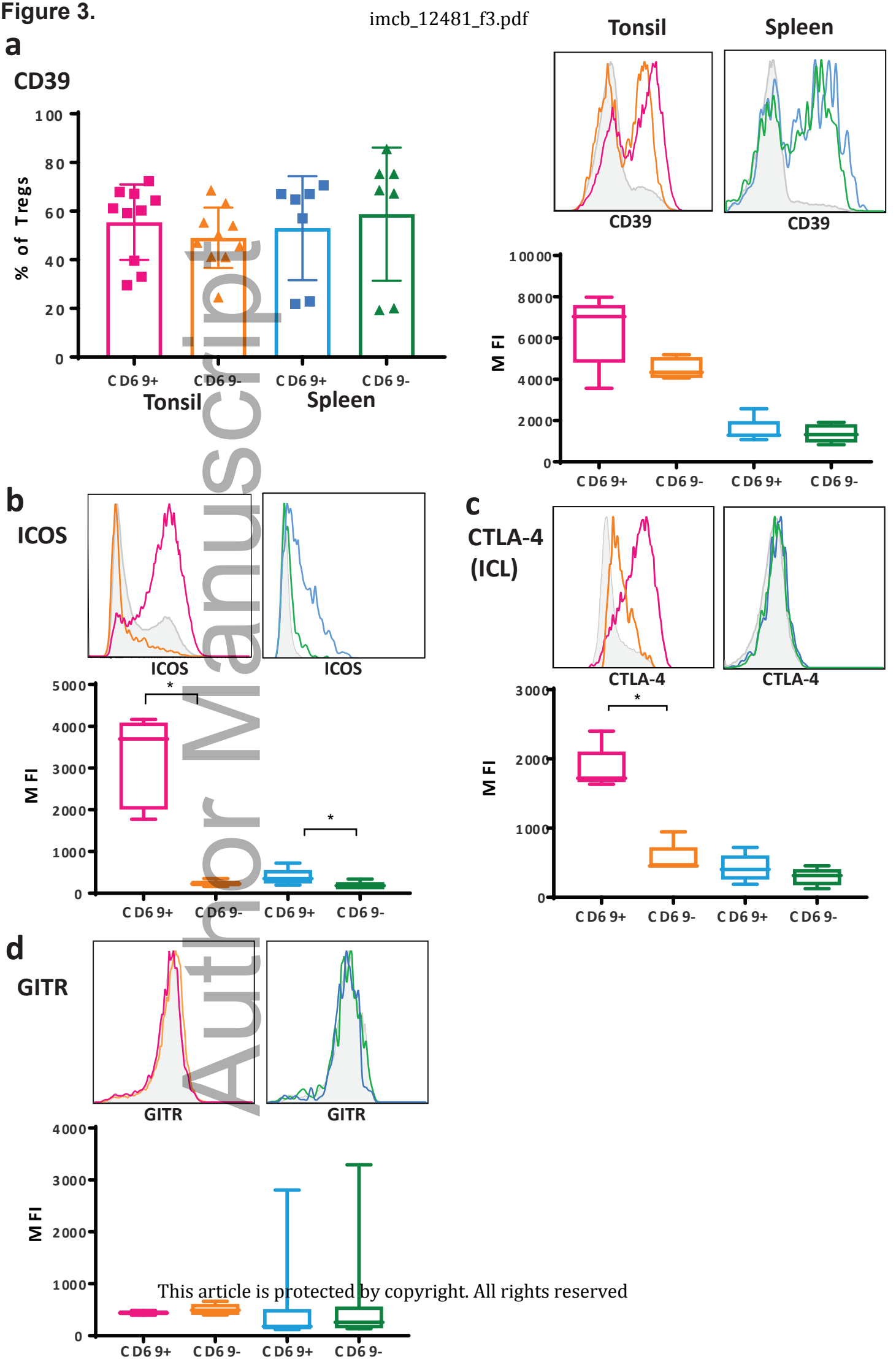

Figure 4.

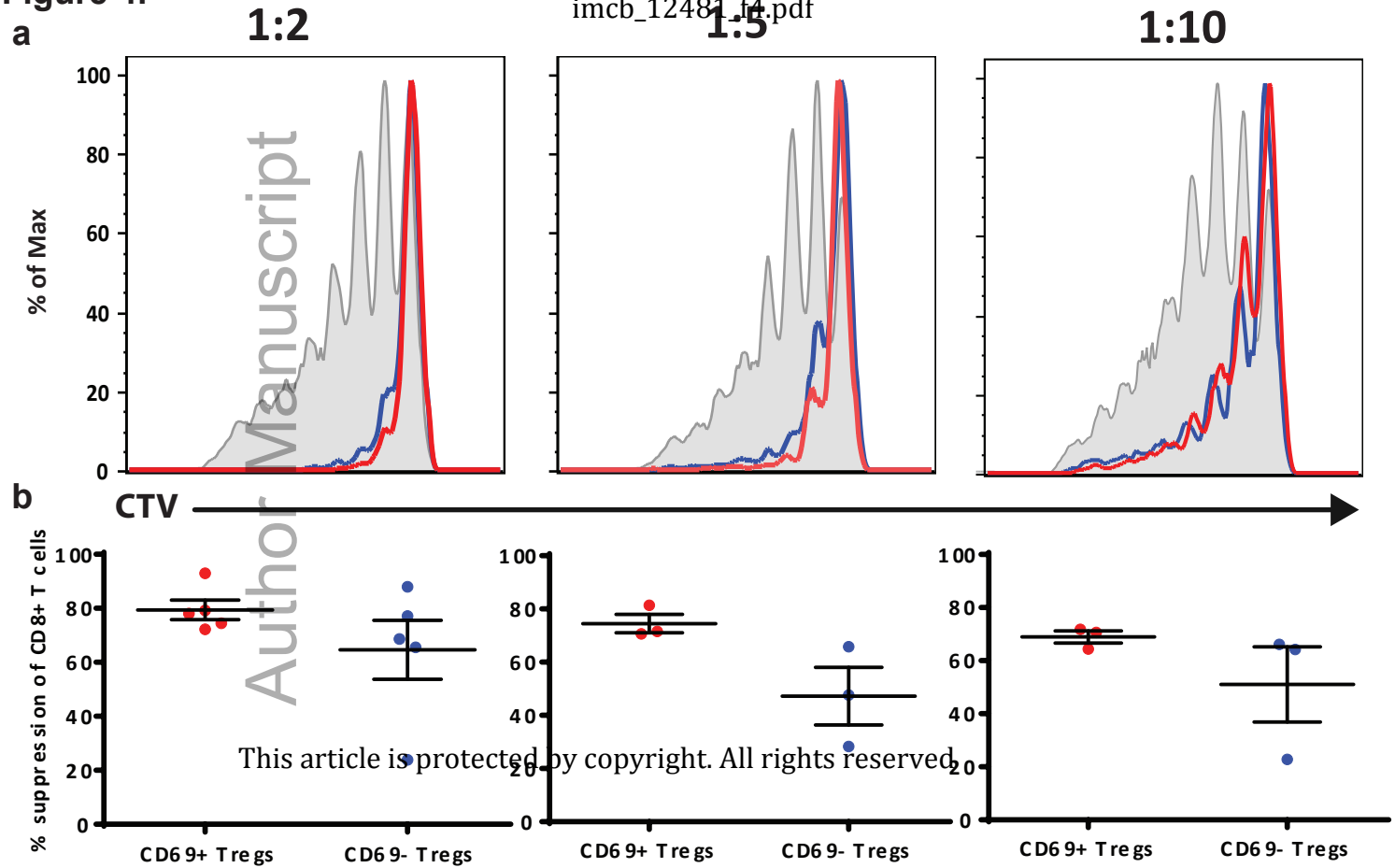

Figure 5.

imcb_12481_f5.pdf

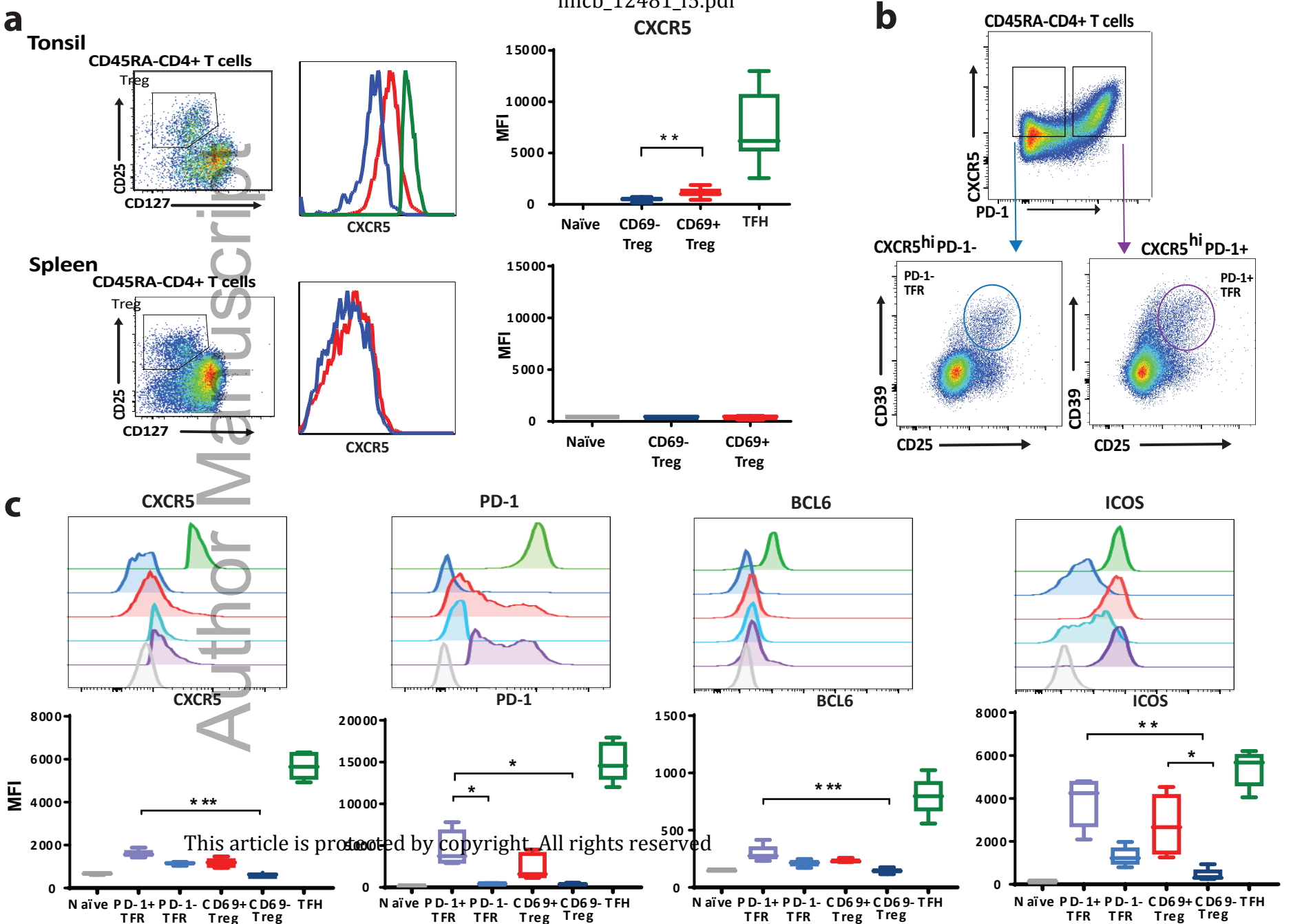

Figure 6.